FUSION OF SATELLITE IMAGES BY SPECTRAL SIGNATURES METHOD

N. Ouarab, Y. Smara, L. Gueciouer & F. Hasnaoui

Laboratory of Image Processing and Radiation. Faculty of Electronics and Computer Sciences.
Houari Boumediene University of Sciences and Technology (USTHB), BP 32 El-Alia, Bab-Ezzouar, 16111 Algiers. ALGERIA -
n.ouarab@lycos.com and y.smara@lycos.com

KEY WORDS: Fusion, FCM classification, Landsat ETM, medium resolution, imaging spectrometer (MeRIS).

ABSTRACT:

Several works of image processing identified the advantage of merging high spectral resolution images with high spatial resolution images, in order to obtain better images and to retrieve more information in several fields of research, such as earth observation research. In this context, we propose, in this paper, the improvement of the spectral resolution of ETM images of Landsat satellite using MeRIS data of ENVISAT satellite. The two characteristics of both images (spatial and spectral) are then preserved.
The technique, inspired from the MMT algorithm approach, is proposed for unmixing the data of a lower resolution by its combined processing with the data of a higher-resolution in order to generate images which have 30 m spatial resolution and 15 spectral bands.
For our work, because some of missing of some data about the Algerian coastal zones and problems of registration between ETM and MeRIS images, we used for this study images from La Camargue (France). For the validation of the results, we retained the evaluation criteria of different parameters. The quality of classification plays a great role in this method (it influences directly on the quality of merged image). The best characteristics of the two images (spatial and spectral) are then preserved in the resulting image.

1. INTRODUCTION

Fusion of multisensor imaging data enables a synergetic interpretation of complementary information obtained by sensors of different spectral ranges (from the visible to the microwave) and/or with different number, position, and width of spectral bands (Richards, 1999) (Minghelli-Roman, 1999) (Minghelli-Roman *and al.,* 2001).
Detailed satellite investigations of the land surface require the spatial resolution of satellite imaging instruments of within a few tens of meters, since due to the land inhomogeneity larger pixels have a high probability to be composed of various classes of land objects. To avoid a significant number of 'mixed' pixels, the resolution of the instrument should be significantly better, than a typical size of homogeneous units.
In this context, the Medium Resolution Imaging Spectrometer (MeRIS) sensor, launched onboard Envisat in 2002, was designed for sea color observation, with a 300-m spatial resolution, 15 programmable spectral bands, and a three-day revisit period. Three hundred meters is a high resolution for an oceanographic sensor, but it is still too rough for coastal water monitoring, where physical and biological phenomena require better spatial resolution. On the opposite, multispectral Landsat Enhanced Thematic Mapper (ETM) images offer a suitable spatial resolution, but have only four spectral bands in the visible and near-infrared spectrum, allowing poor spectral characterization.
One of the possible approaches in a multisensor data environment is to use the data of higher resolution sensors/channels to analyze the composition of mixed pixels in images obtained by lower resolution sensors/channels in order to unmix them.
The purpose of this paper is to present the multisensor multiresolution technique (MMT) proposed by Zhukov (Zhukov *and al.,* 1995, 1996, 1999) and Y.H. Hu (Y.H. Hu *and al.,* 1999). This technique is applied by Minghelli-Roman in order to combine the spectral resolution of MERIS and the spatial resolution of Landsat ETM, the main steps of the method are implemented and the results are presented for the region of La Camargue (France). A validation method is proposed based on different statistical quality criteria.

2. METHODOLOGY

The method is inspired from the MMT (Multiresolution Multisensor Technique). The MMT algorithm is adapted to the practical situation in a multisensor data environment when the detailed spatial information is available only in the high-resolution HR image.
This information is used to analyze composition of the lower resolution LR pixels and to unmix them.
The unmixing of the LR pixels is performed consecutively in the moving window mode. In order to unmix the central LR pixel in the window, contextual information of the surrounding LR pixels is essentially used. In particular, it is assumed that the features, that are recognizable in the high resolution HR image, have the same LR signals in the central LR pixel as in the surrounding LR pixels in the window.
The algorithm includes the following operations as described in figure 1:

- Geometric registration of the two images
- Classification of the HR (ETM) image.
- Definition of class contributions to the signal of the LR (MeRIS) pixels.
- Window-based unmixing of the LR-pixels.
- Reconstruction of an unmixed (sharpened) image.

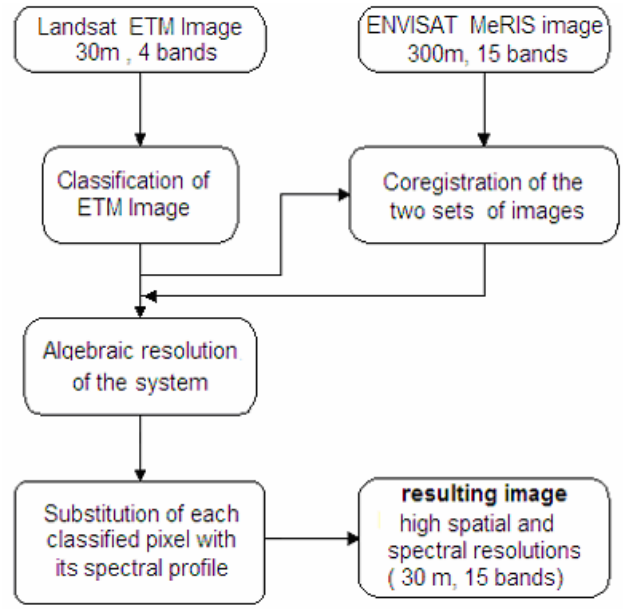

Figure 1. Synopsis

2.1. Image coregistration

First of all, the two images must be geometrically registered. This operation is all the more difficult as the resolution ratio is important. Because this difficulty and some of missing of some data about the Algerian coastal zones, we used for this study images from La Camargue (France) (Courtesy offered by A. Minghelli-Roman). Generally, the lower resolution image is registered on the higher resolution one. The MeRIS image must then be geometrically coregistered on the ETM image.

2.2. Classification of ETM Image

The second step of the algorithm is a classification of the high-resolution LR image (ETM image in our case) into C classes. The first step various unsupervised or supervised algorithms can be used to perform a spectral and/or textural classification of the HR image. The selection of a classification algorithm should depend on a specific application.
In this paper, we will use for this purpose an unsupervised Fuzzy-C Means classification (clustering).

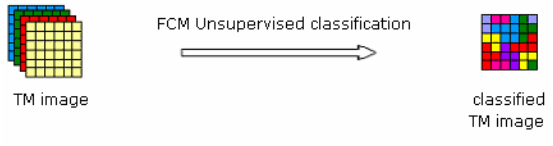

Figure 2. Classification of ETM images

The FCM clustering algorithm is a multivariate data analysis technique and partitions a data set into c ∈ {2,. . ., n-1} overlapping or fuzzy clusters. The partitioning of data into fuzzy clusters is achieved by minimizing the objective function:

$$J_{FCM}(M,C)=\sum_{i=1}^{C}\sum_{j=1}^{N}\left(U_{ij}\right)^{m} d^{2}\left(x_j,C_i\right) \qquad (1)$$

In the equation, M is the membership matrix, C_i is the cluster centers matrix, C is the number of classes, N is the number of data points, and U_{ij} is the degree of membership of sample k in cluster i. The parameter m is a fuzzification parameter that controls the degree of the fuzziness of the resulting classification, which is the degree of overlap between clusters. The choice of m = 2 is widely accepted as a good choice of fuzzification parameter (Güler and Thyne, 2004). The matrix M is constrained to contain elements in the range [0,1] such that:

$$\sum_{i=1}^{c} Uij = 1 \qquad (2)$$

The objective function, J_{FCM}, is minimized by a two-step iteration. First, the C matrix is initialized with random values, and then the M matrix is estimated from the data set, X, m > 1, and C where:

$$U_{ij}=\left(\sum_{k=1}^{C}\left[\frac{d^{2}\left(x_j,C_i\right)}{d^{2}\left(x_j,C_k\right)}\right]^{\frac{1}{m-1}}\right)^{-1} \qquad (3)$$

The FCM algorithm for partitioning can be summarized in the following initialisation steps:

1. Choose a value for the fuzzification parameter, m, with m > 1.
2. Choose a value for the stopping criterion, e (e.g. e = 0.001 gives reasonable convergence).
3. Choose a distance measure in the variable-space (e.g., Euclidean distance).
4. Choose the number of classes C, with C ∈ {2,. ., n-1}.
5. Initialize M = M(0), e.g., with random memberships or with memberships from a hard k-means partition.

For our study, the best values obtained after several tests are 2 for the fuzzification parameter and 0,01 for the stopping criterion.

2.3. Determination of Class Spectra

The third step consists on a calculation of the proportion of each class within each MeRIS pixel (figure 3).
Each MeRIS pixel covers 100 pixels of the ETM classification. The proportion of each class will be calculated within each MeRIS pixel. Let us call P, the vector containing the proportion of each class within a MeRIS pixel.

$$P=\begin{bmatrix} P_1 \\ P_2 \\ \dots \\ \dots \\ P_N \end{bmatrix} \qquad (4)$$

with : $P_i=\dfrac{\sum_{i=1}^{C} pixel\ coded\ i}{r^2} \qquad 0 \le P_i \le 1 \qquad (5)$

where P_i : proportion of the class i in the MeRIS pixel
C : number of classes,
r : ratio of the resolutions of the two images,

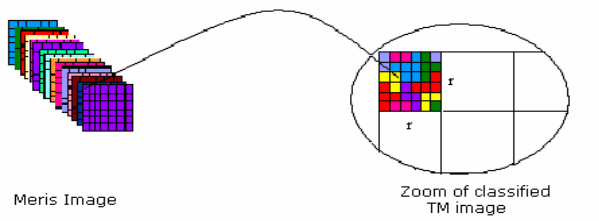

Figure 3. Proportion of each class within each MeRIS pixel

For each class, a mean spectral profile is obtained by solving the following algebraic system :

$$S^i = \sum_{k=1}^{N} P_k L_k^i \qquad 1 \le i \le nb_{MeRIS} \qquad (6)$$

The system can be also written as follows :

$$\begin{bmatrix} S^1 \\ S^2 \\ S^3 \\ \dots \\ S^{nb} \end{bmatrix} = \begin{bmatrix} L_1^1 & L_2^1 & L_3^1 & \dots & L_N^1 \\ L_1^2 & L_2^2 & L_3^2 & \dots & L_N^2 \\ L_1^3 & L_2^3 & L_3^3 & \dots & L_N^3 \\ \dots & \dots & \dots & \dots & \dots \\ L_1^{nb} & L_2^{nb} & L_3^{nb} & \dots & L_N^{nb} \end{bmatrix} \begin{bmatrix} P_1 \\ P_2 \\ P_3 \\ \dots \\ P_N \end{bmatrix} \qquad (7)$$

where S^i : radiance value of the MeRIS spectral band,
N : total number of classes,
P : vector containing the proportion of each class in one MERIS pixel,
L_k^i : unknown vector containing the spectral radiance of each class in the *i*th MeRIS spectral band,
nb_{MeRIS} : number of MeRIS spectral bands.

When the number of equations (nb_{MeRIS}) is lower than the number of unknowns (nb_{MeRIS} x Nc), this matrix system cannot be solved with only one MeRIS pixel but when the number of MeRIS pixels is greater or equals Nc. Since Nc is generally much lower than the number of MeRIS pixels, the number of equations is greater than the number of unknowns, which allows us to refine solutions using the least squares estimator. As a result, the solutions will be less sensitive to the measured radiometric error.

2.4. Output Image Generation

The last step consists of substituting to each classified pixel the corresponding spectral profile obtained by solving the algebraic system. In other words, we generate images which have 30 m spatial resolution and 15 spectral bands.

3. RESULTS AND EVALUATION

For our study, for MeRIS level 2 images of the northern Algeria, we noticed that "black pixels" were located on land–water borders (Algerian coastal zones). These mixed pixels are not corrected and their MeRIS level 2 reflectance is set to zero for all spectral bands. For this reason, we have had some problems of registration between ETM and MeRIS images, and then images over La Camargue (Southern France) are used for this study (Minghelli-Roman *and al*., 2004). For the validation of the results, we retained the evaluation criteria of the following parameters : correlation coefficient and the average quadratic error. We carried out several tests to specify the parameters which lead to the final result. The quality of classification plays a great role in this method (it influences directly on the quality of merged image). The final result is obtained only after the execution of several tests, and long experiments, to lead to a result which comprises high spatial and spectral resolutions at the same time. The best characteristics of the two images (spatial and spectral) are then preserved in the resulting image (figures 6 to 9).

For validation purposes, the resulting image bands have been compared to the corresponding ETM spectral bands in order to optimize the number of classes.

3.1. Coefficient of correlation Cr

Regarding the figures 4a and 4b, we can remark that the 15 MeRIS bands are contained in the same spectral range that the range from the ETM 1 up to ETM 4 bands. Then, we can apply the multispectral classification (FCM) with only the spectral bands 1, 2, 3, et 4 of ETM data which are situated in the visible and the near infrared domains.

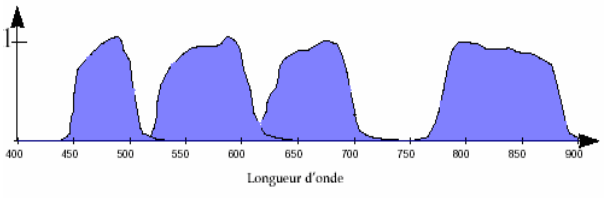

a. Spectral range of ETM data

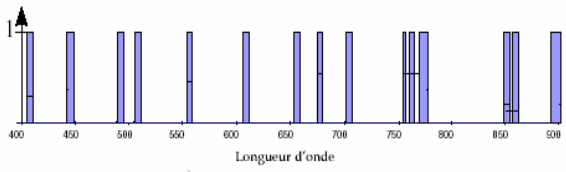

b. Spectral range of MeRIS data

Figure 4: Spectral range of the two images ETM and MeRIS

Then :

- ETM1 → MeRIS (band2 & band3).
- ETM2 → MeRIS (band4, band5 & band6).
- ETM3 → MeRIS (band7, band8 & band9).
- ETM4 → MeRIS (band12, band13, band14 & band15).

From the merged image (i.e. 15 bands of spatial resolution of 30 m), we generate the M image with four bands as follows :

- Band M1: mean of bands 2 & 3 of merged image (pixel to pixel).
- Band M2: mean of bands 4, 5 & 6 of merged image (pixel to pixel).
- Band M3: mean of bands 7, 8 & 9 of merged image (pixel to pixel).
- Band M4: mean of bands 12, 13 & 14 of merged image (pixel to pixel).

We calculate the coefficient of correlation between the bands :

- Cr1 = correlation (M1, ETM1).
- Cr2 = correlation (M2, ETM2).
- Cr3 = correlation (M3, ETM3).
- Cr4 = correlation (M3, ETM3).

The coefficient of correlation inter bands is given by :

$$Cr_i(x, y) = \frac{E[(x - \bar{x})(y - \bar{y})]}{\sqrt{E[(x - \bar{x})^2]\,E[(y - \bar{y})^2]}} = \frac{Cov(x, y) - m(x)m(y)}{\sigma(x) * \sigma(y)} \quad (8)$$

Where x : pixel value in the band X,
y : pixel value in the band Y,
E : Mean,
$\bar{x}$: Mean of the variable x in the band X,
$\bar{y}$: Mean of the variable x in the band Y.

and the total coefficient of correlation is:

$$Cr = \frac{\sum_{i=1}^{4} Cr_i}{4} \quad (9)$$

The variation of the coefficient of correlation with the number of classes is given by the figure 5.

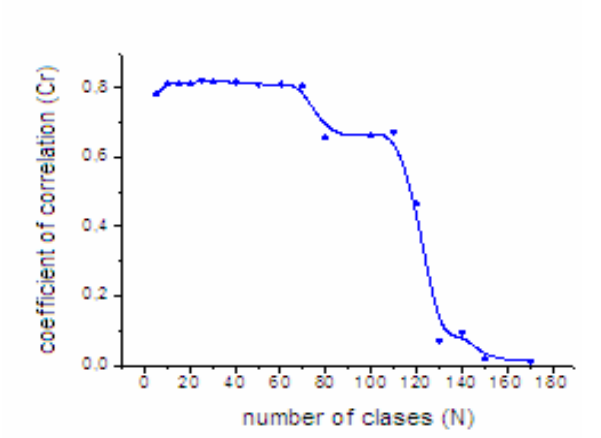

Figure 5. variation of the coefficient of correlation

The function gives a maximum from the number of classes N=25 up to N=65.

3.2. Root mean square error (RMSE)

The criterion chosen for this comparison is the root mean square error (RMSE) error which depends on the mean and standard deviation differences

$$RMS_i = \sqrt{m_{diff}^2 + \sigma_{diff}^2} \qquad 1 \le i \le 4 \quad (10)$$

The mean is given by :

$$m = \frac{\sum_{i=1}^{n} L(x_i, y_i)}{n} \quad (11)$$

The standard deviation is given by :

$$\sigma = \sqrt{\frac{1}{n}\sum_{i=1}^{n}(L(x_i, y_i) - m)^2} \quad (12)$$

Where $L(x_i, y_i)$: Luminance of pixel (x_i, y_i),
n : Number of pixels in the image.

The total root square mean error is given by :

$$RMS = \frac{\sum_{i=1}^{4} RMS_i}{4} \quad (13)$$

For all images, Classifications have been applied on the ETM image with different numbers of classes (namely 30, 40, 50, 60, 100 and 200 classes) in order to assess the influence of this number of classes on the fusion output. For our case, the error is minimum for 60 classes.

The method described above has been applied to ETM and MeRIS images. The figure 6 shows a color composite of the input MeRIS image. A zoom factor of 10 has been applied to this image in order to emphasise the difference between the ETM and MeRIS resolutions. The figure 7 shows the unsupervised classification (FCM method) with 60 classes obtained from the ETM image. The input ETM color composite image is shown in the figure 8.

Finally, the resulting image, in the figure 9, is characterized by 15 spectral bands and a 30 m resolution. A spatial improvement can be noted by comparing between Figures 6 and 9.

Figure 6. MeRIS color composite image (300 m, 15 spectral bands).

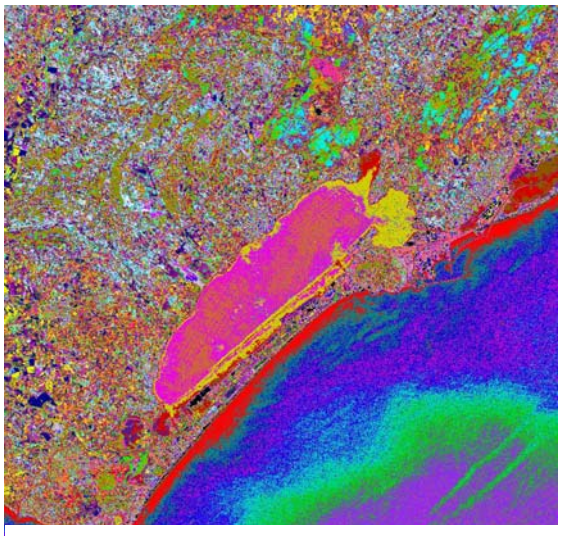

Figure 7. Result of classification with 60 classes applied on the Thematic Mapper image

Figure 8. Thematic Mapper color composite (30 m, six spectral bands).

Figure 9. Resulting image color composite (30 m, 15 spectral bands).

3. DISCUSSIONS AND CONCLUSION

The application of the MMT unmixing to a ETM image as well as to a MeRIS image has demonstrated a significant improvement in sharpness and radiometric accuracy in comparison to the original images.

The analysis of the MMT sensitivity to sensor errors showed that the strongest requirement is the accuracy of geometric coregistration of the data; the coregistration errors should not exceed 0.1–0.2 of the linear pixel size of the low-resolution image. This is a strong but not unrealistic requirement to modern coregistration techniques

This communication has shown how a MeRIS image can be merged with a ETM image in order to synthesize a new product with the best characteristics of each sensor: the spatial resolution of ETM images, and the spectral resolution and the revisit frequency of MeRIS images.

ACKNOWLEDGEMENTS

This study was performed in the framework of ESA project AOE 703. A. Minghelli-Roman is acknowledged for providing the data set (ETM and MeRIS) over La Camargue (France) for the study and ESA is acknowledged for providing help and the algerian MeRIS data which will be used after good co-registration.

REFERENCES

Güler, C., & Thyne, G.D.,2004. Delineation of hydro chemical acies distribution in a regional groundwater system by means of fuzzy c-means clustering. *Water Resour. Res.*, 40, W12503, doi:10.1029/2004WR003299.11p.

Hu, Y.H., Lee, H.B., & Scapace, F.L., 1999. Optimal linear spectral unmixing. *IEEE Trans. Geosci. Remote Sens.*, Vol 37, pp 639-644.

Minghelli-Roman, A., 1999. Apport et perspectives de l'imagerie hyperspectrale pour la télédétection des paysages natures et Agricoles," *Ph.D. dissertation,* Univ. Nice Sophia-Antipolis, France.

Minghelli-Roman, A., Mangolini, M. M., Petit, M., and Polidori, L., 2001. Spatial resolution improvement of MeRIS images by fusion with ETM images. *IEEE Trans. Geosci. Remote Sens.*, vol. 39, no. 7, pp. 1533–1536.

Minghelli-Roman, A., Marni, S., Cauneau, F., & Polidori, L., 2004. Conception of products and services For coastal applications. *EARSeL eProceedings* 3, 2.

Richards, J. A., 1999. *Remote Sensing Digital Image Analysis. An Introduction.* Berlin, Germany: Springer-Verlag. 363 p.

Zhukov, B., Oertel, D., 1995. A technique for combined processing of the data of an imaging spectrometer and of a multispectral camera," *Proc.SPIE*, vol. 2480, pp. 453–465.

Zhukov, B., Oertel, D., 1996 . Multi-sensor multi-resolution technique and its simulation. *Zeitschrift Photogramm. Fernerkundung*, no. 1, pp. 11–21.

Zhukov, B., Oertel, D., Lanzl, F. & Reinhackel, G., 1999. Unmixing-based multi sensor multi-resolution image fusion. *IEEE Trans. Geosci. Remote Sens.*, Vol 37, pp 1212-1236.